BJR

https://doi.org/10.1259/bjr.20190089

Received: 23 January 2019 | Revised: 11 March 2019 | Accepted: 18 March 2019

Cite this article as:
Wang T, Press RH, Giles M, Jani AB, Rossi P, Lei Y, et al. Multiparametric MRI-guided dose boost to dominant intraprostatic lesions in CT-based High-dose-rate prostate brachytherapy. *Br J Radiol* 2019; **92**: 20190089.

FULL PAPER

Multiparametric MRI-guided dose boost to dominant intraprostatic lesions in CT-based High-dose-rate prostate brachytherapy

TONGHE WANG, PhD, ROBERT H. PRESS, MD, MATT GILES, MS, ASHESH B. JANI, MD, PETER ROSSI, MD, YANG LEI, PhD, WALTER J. CURRAN, MD, PRETESH PATEL, MD, TIAN LIU, PhD and XIAOFENG YANG, PhD

Department of Radiation Oncology and Winship Cancer Institute, Emory University, Atlanta, GA, USA

Address correspondence to: Dr Xiaofeng Yang
E-mail: *xyang43@emory.edu*

Objective: The purpose of this study is to investigate the dosimetric feasibility of delivering focal dose to multiparametric (mp) MRI-defined DILs in CT-based high-dose-rate (HDR) prostate brachytherapy with MR/CT registration and estimate its clinical benefit.
Methods: We retrospectively investigated a total of 17 patients with mp-MRI and CT images acquired pre-treatment and treated by HDR prostate brachytherapy. 21 dominant intraprostatic lesions (DILs) were contoured on mp-MRI and propagated to CT images using a deformable image registration method. A boost plan was created for each patient and optimized on the original needle pattern. In addition, separate plans were generated using a virtually implanted needle around the DIL to mimic mp-MRI guided needle placement. DIL dose coverage and organ-at-rick (OAR) sparing were compared with original plan results. Tumor control probability (TCP) was estimated to further evaluate the clinical impact on the boost plans.
Results: Overall, optimized boost plans significantly escalated dose to DILs while meeting OAR constraints. The addition of mp-MRI guided virtual needles facilitate increased coverage of DIL volumes, achieving a V150 > 90% in 85 % of DILs compared with 57 % of boost plan without an additional needle. Compared with original plan, TCP models estimated improvement in DIL control by 28 % for patients with external-beam treatment and by 8 % for monotherapy patients.
Conclusion: With MR/CT registration, the proposed mp-MRI guided DIL boost in CT-based HDR brachytherapy is feasible without violating OAR constraints, and indicates significant clinical benefit in improving TCP of DIL. It may represent a strategy to personalize treatment delivery and improve tumor control.
Advances in knowledge: This study investigated the feasibility of mp-MRI guided DIL boost in HDR prostate brachytherapy with CT-based treatment planning, and estimated its clinical impact by TCP and NTCP estimation.

INTRODUCTION

Current prostate high-dose-rate (HDR) brachytherapy treats the whole prostate gland with one prescribed dose level since prostate cancer is known to be multifocal.[1–5] However, dominant intraprostatic lesions (DILs) are commonly identified in prostate cancer histopathologic studies. A single or few DILs provide the large majority of the tumor burden despite typically representing less than 10% of the total gland volume. Importantly, the DIL is the most common sites of recurrence after radiation therapy.[6–8] Studies show that selectively escalating the dose to DILs has the potential to increase tumor control probability with low toxicity.[9,10] Thus, it is desirable to dose escalate DILs during whole prostate HDR brachytherapy.

Routine DIL boost, however, is not performed due to several challenges. First, it requires accurate definition of DIL location and size. Recent advances in multiparametric MRI (mp-MRI) have shown efficacy in identifying DILs,[11–14] of which the reliability, accuracy, and reproducibility are validated by pathology gold standards.[15–18] Thus, it is promising to provide image guidance for treatment planning in external-beam radiation therapy (EBRT) or HDR brachytherapy for DIL boost.[19,20] Secondly, accurate image registration is needed between the mp-MRI images and CT simulation images to provide DIL contours for plan optimization and dose evaluation for CT-based brachytherapy. Registration of the mp-MRI with live transrectal ultrasound (TRUS) images at the time of needle placement would also be valuable in order to optimize the

dose coverage. Accurate multimodality registrations between mp-MRI and TRUS, and between mp-MRI and CT are critical for precise boost treatment planning. Recently, sophisticated image registration methods between MRI and TRUS, and between MRI and CT, has been proposed and validated in accuracies,[21,22] which addressed the current implementation difficulties in clinical application.

In the step of needle implanting, dose escalation to DILs can be achieved by optimizing plans either based on standard needle pattern or with image guided needle placement in and around the DIL. Recent studies introduced DIL boost planning based on the optimization of standard whole prostate needle placement without additional targeted needles.[6] Registration between mp-MRI and TRUS may be avoided in this method, however dose coverage would be expected to be worse than with the addition of targeted boost needles.[23] Other studies proposed DIL boost planning with additional needles solely based on TRUS using rigid registration with mp-MRI and demonstrated successful focal boost dose delivered without violating normal tissue constraints.[10,23] However, rigid registration has limited accuracy since the TRUS is acquired at a different patient position than the MRI, and the ultrasound probe may deform the prostate gland.[24] In addition, the TRUS images have low image quality and spatial resolution and thus may have inferior performance compared with CT for organs-at-risk (OARs) contouring and especially for needle reconstruction.[25] Moreover, although the dose boost feasibility is verified, its clinical benefit and impact remains unknown.

In this study, we investigated the feasibility and potential clinical impact of DIL dose boost in HDR brachytherapy based on CT simulation treatment planning, with a newly developed deformable registration method between mp-MRI and CT.[22] The purpose of this study was to determine the extent to which the DIL could be boosted while maintaining OAR sparing and prostate coverage, and to estimate its clinical benefit. In the cohort of 17 patients with 21 DILs, we retrospectively evaluated the dose coverage of DILs in treatment plans with added virtual boost needles and compared OAR sparing and prostate coverage with original plans. Tumor control probability (TCP) and normal tissue complication probability (NTCP) were estimated to further evaluate the clinical impact on the boost plans.

METHODS AND MATERIALS

Patients

We retrospectively reviewed a total of 17 patients with prostate HDR brachytherapy treated in our clinic. Median age was 67 (range 45–79), clinical stage ≤T2a, median PSA was 7 (range 0.9–20), median prostate volume was 53.3 cc measured on CT (range 25.1cc-124.9cc), and Gleason score was six or 7. Eight patients received a boost (15 Gy ×1) after 45 Gy EBRT in 25 fractions to the prostate and seminal vesicles, and nine received monotherapy (13.5 Gy ×2). Institutional review board approval was obtained with no informed consent was required for this HIPAA-compliant retrospective analysis.

Figure 1. Example of DIL delineation on T_2 weighted MRI (left) and ADC map (right).

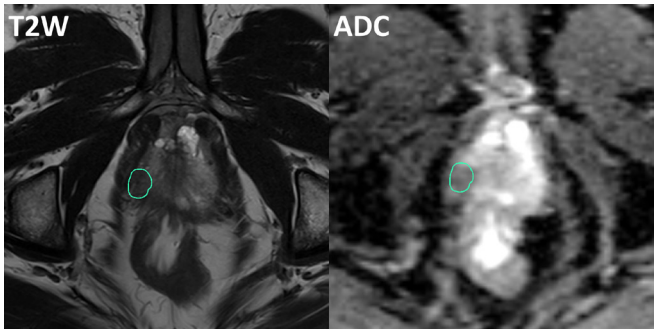

Image acquisition and contouring

Mp-MRI scans were performed on average 3 months before HDR treatment, which included T_1 weighted, T_2 weighted and diffusion weighted MRI. Scans were performed on a TrioTim (Siemens, Germany) 3T scanner. T_1 weighted MRI used turbo-spin echo (SE) sequence with repetition time (TR) 1240 ms, echo time (TE) 10 ms, echo train length 3, 0.8 mm pixel size and 3 mm slice thickness. T_2 weighted MRI used SE sequence with TR 3480 ms, TE 101 ms, echo train length 20, 0.31 mm pixel size and 3 mm slice thickness. DWI MRI used a single-shot SE-echo planar imaging (EPI) with TR 6311 ms, TE 89 ms, 1.88 mm pixel size and 3 mm slice thickness. Apparent diffusion coefficient (ADC) maps were then generated for analysis. DILs were contoured based on the above MRI images in VelocityAI 3.2.1 (Varian Medical Systems, Palo Alto, CA), and consensus was achieved by two radiation oncologists (RP and PP). An example of DIL delineation on T_2 weighted MRI and ADC map is shown in Figure 1. Each patient has at least one DIL found within prostate, and the average DIL volume among the 17 patients is 1.75 ± 1.12 cc (range 0.22–4.35cc).

In the delivered HDR treatment, 12–18 (depending on prostate size) Nucletron ProGuide Sharp 5F needles were placed under TRUS guidance. CT images were acquired after needle implantation by Brilliance Big Bore (Philips, Netherlands) with 140 kVp, 350 mAs, 0.5 mm pixel size and 1 mm slice thickness. On CT images, physicist reconstructed needles, and radiation oncologist delineated the whole prostate as PTV, and OARs including bladder, rectum, and urethra.

Deformable registration

In this treatment planning study, deformable image registration was applied through in-house code between mp-MRI and CT images to propagate the consensus DIL contours from mp-MRI to CT images. Conventional intensity-based deformable registration method has limited accuracy due to the intrinsic differences in grey-level intensity characteristics between the two modalities as well as the presence of low contrast between prostate and surrounding soft tissues in CT images. We have already developed a dictionary-learning-based deformable registration method, and a clinical study demonstrated that our method outperformed current intensity-based registration method. The related study on this deformation method developed by our group has been published,[22] and will be briefly introduced here.

In this method, a number of training MR and CT images (21 in our study) are first registered offline by the state-of-the-art registration algorithms[26–30] with finely tuned parameters and manually annotated landmarks. A set of deformation fields is then obtained from these training datasets and construct a dictionary. For any MR and CT images of a new patient, we assume that any image patch in the new MR image can be well represented by a sparse linear combination of similar patches from the training images. The registration can be completed by the following five steps. (1) A set of key points are first selected automatically in the new CT image. (2) A coupled dictionary is adaptively constructed for each key point, where each coupled element in the dictionary consists of a pair of patch-based image appearance and its associated deformation between training MR and CT image. (3) Given the local dictionary at each key point, the patch on new CT image around that key point can be expressed as a sparse linear combination of neighboring patches from the training CT images. The combination coefficients are solved in an optimization framework with sparse regularization. The initial deformation on each key point of a new MRI is then predicted as the linear combination of deformations from dictionary with the corresponding solved coefficients. (4) Based on the estimation of the initial deformations on the key points of the subject image, B-spline is applied to interpolate the initial deformation field for the whole MR image. (5) The MR image is deformed by following the predicted deformation field. Patient studies show that the registration error of this method is less than 2 mm. Thus, 2 mm margin was added on DIL contours to include such uncertainty of registration.

Treatment planning study

To validate the feasibility of DIL dose boost and examine the benefit of implanting additional needles around DILs, we compared the following three scenarios: The first scenario is the clinical treatment plan delivered on each patient with the original needle placement determined on CT images. The plan was optimized to achieve prescribed coverage on whole prostate (D90 >100%, V100 >90% of prescribed dose) and spare dose on OARs (OAR constraints used were: Bladder and Rectum V75 <1 cc, Urethra V125 <1 cc and Urethra D10 <118 %).[31] DILs were not considered in optimization in this current clinical HDR planning. The second scenario is the treatment plan with original needle pattern but re-optimized for additional dose coverage of DILs. The third scenario is the treatment plan with original needle pattern and one virtual needle added near each DIL. For scenario 2 and 3, the dose distribution was re-optimized to maximize the DIL volume receiving 150% of the whole prostate prescription dose while meeting OAR constraints. In the following context, we refer to the above three scenarios as "Original", "Original Boost", and "Additional Boost", respectively. Note that although each of monotherapy patient has two separate implants, the implant patterns are usually same, thus only the first treatment is included in this study. The treatment planning system was Oncentra 4.5.3 (Elekta, Stockholm, Sweden). Clinically relevant DVH metrics were selected for comparison among the three scenarios on prostate with DIL cropped, DIL, bladder, rectum and urethra. A Wilcoxon signed-rank test was performed between "Original" *vs* "Original Boost", and "Original" *vs* "Additional Boost" to evaluate the significance of corresponding dose coverage improvement on DIL. Such test was also performed between "Original Boost" and "Additional Boost" to assess the necessity of additional needles. A p value < 0.05 was considered as statistically significant.

TCP and NTCP modeling

To further evaluate the clinical impact of boost plans, we examined the tumor control probability (TCP) and normal tissue complication probability (NTCP). First, the dose in DVH was converted to equivalent dose in 2 Gy/fraction (EQD_2) based on the linear quadratic model.[32,33] For the DVH of prostate or DIL which has the jth bin of volume v_j receiving dose d_j each fraction to total dose D_j , TCP was calculated using the LQ-Poisson Marsden model,[34] which is defined as

$$TCP = \frac{1}{\sigma_\alpha\sqrt{2\pi}}\int_0^\infty \prod_j \exp\left[-\rho_{clon} v_j \exp\left(\alpha D_j\left(1+\frac{\beta}{\alpha}d_j\right)\right)\right]\cdot\exp\left[-\frac{\left(\alpha-\bar{\alpha}\right)^2}{2\sigma_\alpha^2}\right]d\alpha \quad (1)$$

Eq. (1) assumes the population of clonogenic cells (with initial cell density ρ_{clon} and constant α/β ratio) has radiosensitivity (α) varies according to a gaussian distribution with mean $\bar{\alpha}$ and standard deviation σ_α . In this study, we investigated three cases with different α/β ratios (1.5 Gy, 3 Gy and 10 Gy) for prostate and DIL, each of which corresponds to a different set of parameters ($\bar{\alpha}$ and σ_α) as publications.[35,36] Note that EQD_2 was also calculated separately for each α/β ratio. ρ_{clon} in DIL and non-DIL was assumed to be 1×10^7 /cc and be 6.2×10^4 / cc respectively as references[36,37] for all α/β ratios.

NTCP was calculated for bladder, rectum and urethra by Lyman-Kutcher-Burman model with Niemierko's equivalent uniform dose,[38–40] which is defined as

$$NTCP = \frac{1}{\sqrt{2\pi}}\int_{-\infty}^{t}\exp\left(-x^2/2\right)dx \quad (2)$$

where $t = \frac{EUD-TD_{50}}{mTD_{50}}$. TD_{50} is the dose resulting in 50% probability of complication in a uniformly irradiated tissue, and m is inversely proportional to the dose-complication slope. EUD is equivalent uniform dose, which is defined as

$$EUD = \sum_j\left(D_j^{\frac{1}{n}}\frac{v_j}{v_{total}}\right)^n \quad (3)$$

where n is OAR-dependent parameter and v_{total} is the total volume of that OAR. The parameters TD_{50} , m and n were chosen according to existing studies. All the parameters for TCP and NTCP calculation are listed in Tables 1 and 2. The calculation was implemented by Biosuite software.[35] For patients who had EBRT before HDR, the dose received from EBRT was included with HDR dose together in calculation, and were analyzed separately from monotherapy patients. Note that prostatic urethra was not routinely visualized, contoured or used as a dose limiting structure in EBRT, thus it was assumed to have full prescription dose in whole volume during the NTCP calculation.

Table 1. TCP parameters

α/β(Gy)		$\bar{\alpha}(Gy^{-1})$	$\sigma_\alpha(Gy^{-1})$	$\rho_{clon}(cc^{-1})$
1.5	Prostate-DIL[a]	0.155	0.058	6.2×10^4
	DIL	0.155	0.058	1×10^7
3	Prostate-DIL	0.217	0.082	6.2×10^4
	DIL	0.217	0.082	1×10^7
10	Prostate-DIL	0.301	0.114	6.2×10^4
	DIL	0.301	0.114	1×10^7

[a]Prostate - DIL = Prostate with DIL cropped.

RESULTS

In Figure 2, the dose distributions of original plan, boost plan and boost plan with additional needles were compared side-by-side-for one patient as an example. In original plan, DIL received mostly the prescription dose of prostate. The "Original Boost" plan successfully deposited boost dose to the part of DIL close to one of the original needle (V150 = 83.0% DIL coverage) but further dose escalation was limited in this needle geometry due to OAR constraints. The "Additional Boost" with an additional needle around DIL achieved the highest DIL V150 coverage (V150 = 97.2%) among the three plans. The DVH comparison on this patient was shown in Figure 3. The dose deposited in the DIL was significantly increased from the original to the boost, and increased further with the additional needle. For non-DIL prostate region and OARs, the DVH curves did not vary significantly among the three plans.

The comparison of DVH metrics on prostate and DIL among the three plans in the cohort of 17 patients were summarized in Table 3. For non-DIL prostate region, no significant differences were found except "Original" *vs* "Original Boost" in V100 and V200: "Original Boost" showed 1% less 100% prescription dose coverage and 1.1% larger hotspot of >200% prescription dose than "Original" on average with statistical significance. For DIL, both boost plans has significant dose increase compared with original plan. "Additional Boost" significantly outperformed "Original Boost" in D90, V150, V175 and V200. Figure 4 showed the percentage of DILs with different dose coverage in the three plans. "Additional Boost" was able to escalate dose to V150 >90% among 85% of DILs and V175 >90% among 35% of DILs, which was 30% higher than those of "Original Boost". These results are consistent with the above qualitative findings and quantitatively demonstrate dose coverage improvement on DIL by additional needle.

Similar comparison of OARs was summarized in Table 4. Statistically significant differences were found in rectum D2cc and urethra V125 between original plan and both the two boost plans: 0.24 and 0.31% of prescription dose increase in D2cc of rectum, and 0.03 cc and 0.02 cc increases in V125 of urethra for "Original Boost" and "Additional Boost", respectively. There was no significant difference between the two boost plans on rectum D2cc and urethra V125.

Figure 2. Dose distributions of "Original", "Original Boost" and "Additional Boost" plans. Prostate and DIL are indicated by red and blue contours. The original needle pattern is marked by blue dots in top left. The additional needle is marked as white cross-in bottom right.

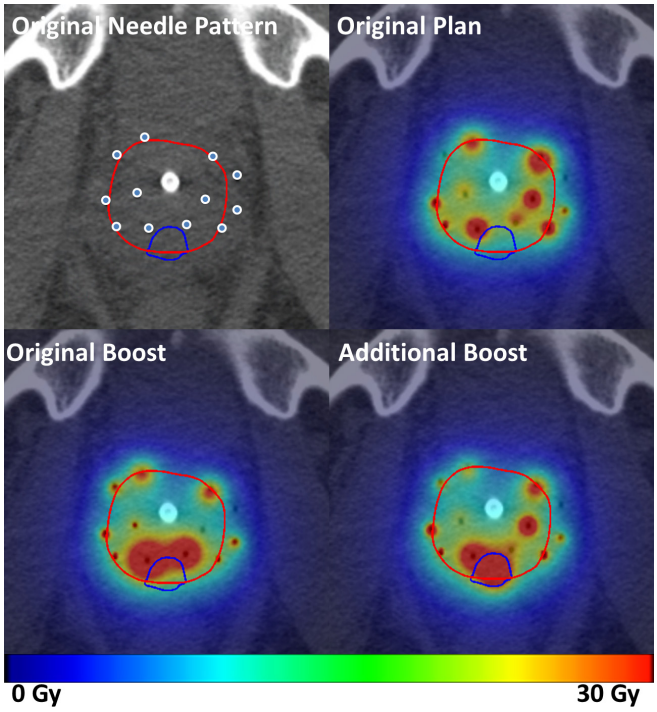

The TCP and NTCP results were summarized in Table 5. Overall, the two boost plans both significantly increased the TCP of DILs compared to the original plan, while maintaining the TCP of non-DIL prostate region without significant difference. The increase in DIL TCP was greater for patients with prior EBRT compared to monotherapy patients. For "Additional Boost", such gains were ~30% compared to less than 10% for monotherapy patients when α/β=1.5. For monotherapy patients, DIL TCP improvement by "Additional Boost" for α/β=10 (21.8%) was more than twice higher than that for α/β=1.5 (7.8%), while for patients with EBRT, they were about the same. "Additional Boost" outperformed "Original Boost" in DIL TCP for all cases, and the larger benefit of "Additional Boost" over "Original Boost" was also on patients with EBRT when α/β=1.5 (6.5%), α/β=3 (9.3%) and α/β

Table 2. NTCP parameters

		α/β(Gy)	TD_{50}(Gy)	*m*	*n*	Source
Bladder	Contracture/volume loss	3	76.9	0.13	0.09	Burman, et al.[41]
Rectum	Grade 2 + late toxicity or rectal bleeding	3	80.0	0.11	0.5	Michalski, et al.[42]
Urethra	Stricture requiring urethrotomy within 4 years after RT completion	5	70.7	0.37	0.3	Panettieri et al.[43]

Figure 3. The DVHs of patient in Figure 1 of "Original", "Original Boost" and "Additional Boost" plans. Prostate-DIL = Prostate with DIL cropped.

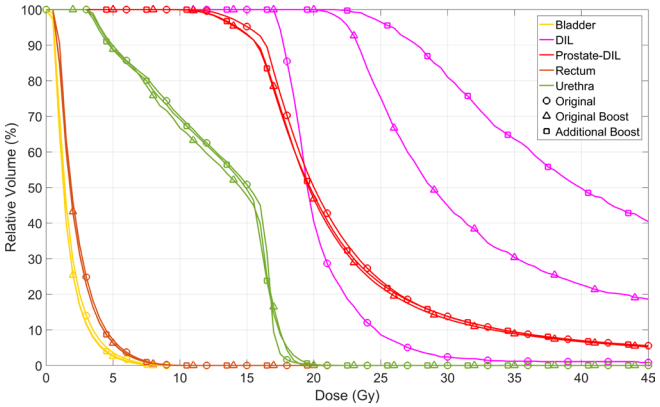

=10 (13.3%) compared with monotherapy patients (1.2%, 1.8 and 4.5% for α/β=1.5, 3 and 10, respectively).

NTCP results for bladder and rectum had no significant difference among all the three plans for all cases. On urethra, the two boost plans showed 0.8–1.1% ($p < 0.05$) and 2.3–2.8% ($p < 0.05$) higher NTCP for patients with EBRT and monotherapy patients, respectively. No significant difference was shown between the "Additional Boost" and "Original Boost" in urethra NTCP.

DISCUSSION

In this study, we investigated the feasibility of mp-MRI-guided DIL boost in HDR prostate brachytherapy with CT-based treatment planning, and estimated its clinical impact by TCP and NTCP estimation. Boost plans, both with and without additional needles, significantly escalated dose to DILs while maintaining OAR constraints. Compared with boost plans using original needle placement, the boost plans with additional needles achieved DIL dose coverage of 150% or 175% of prescription dose in 30% more cases. This resulted in an increase in DIL TCP by 28% for patients with EBRT and by 8% for monotherapy patients from original plan (when α/β=1.5). The dose to non-DIL prostate and bladder remained unchanged. Rectal and urethral

Figure 4. Percentage of DILs receiving different dose coverage in different plans.

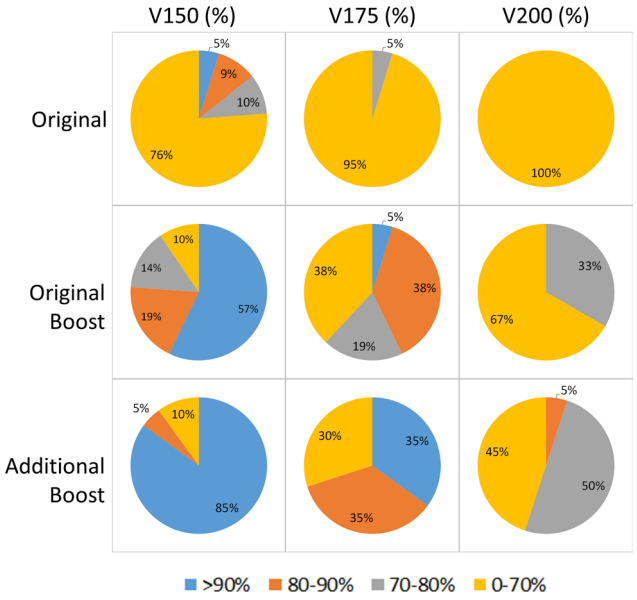

doses were slightly increased, but only urethra demonstrated an increase in NTCP (<3%).

The potential clinical utilities of mp-MRI in guiding HDR brachytherapy are twofold: guiding needle placement on TRUS around DILs in real time during the implantation and guiding treatment planning on CT to boost dose on DILs. Our previous studies proposed sophisticated image registration methods for mp-MRI *vs* TRUS and mp-MRI *vs* CT and validated their accuracies,[21,22] which addressed the current implementation difficulties in clinical application. This study aimed to evaluate the potential clinical significance of mp-MRI-guided DIL boost plans, and to present the value of mp-MRI-guided needle placement by demonstrating the dosimetric advantages of additional needle over standard needle placement. This study, along with a series of our previous studies, develops a feasible strategy to personalize the treatment delivery for HDR prostate patients and improve their tumor control probability.

Table 3. DVH metrics of prostate and DIL in different plans among all 17 patients.

	Prostate-DIL[a]				DIL				
	D90(%)	V100(%)	V150(%)	V200(%)	D90(%)	V100(%)	V150(%)	V175(%)	V200(%)
I[b]	106.6 ± 1.7	94.7 ± 1.2	35.9 ± 3.7	14.0 ± 1.7	114.6 ± 21.9	94.4 ± 9.7	46.4 ± 28.6	26.3 ± 21.4	19.1 ± 16.6
II	105.5 ± 2.6	93.7 ± 1.7	37.1 ± 4.0	15.1 ± 1.9	151.6 ± 22.8	98.7 ± 4.8	87.0 ± 15.5	69.3 ± 20.9	52.9 ± 21.9
III	106.3 ± 3.1	93.9 ± 1.9	37.1 ± 4.0	14.6 ± 2.1	164.5 ± 21.1	99.4 ± 2.5	93.0 ± 14.1	79.5 ± 18.6	65.2 ± 16.8
P-values									
I *vs* II	0.149	0.049	0.163	0.015	<0.001	<0.001	<0.001	<0.001	<0.001
I *vs* III	0.979	0.326	0.215	0.070	<0.001	<0.001	<0.001	<0.001	<0.001
II *vs* III	0.393	0.836	0.717	0.179	0.001	0.250	<0.001	0.002	0.020

[a]Prostate - DIL = Prostate with DIL cropped.
[b]I, II and III are "Original", "Original Boost" and "Additional Boost" plans, respectively.

Table 4. DVH metrics of OARs in different plans among all 17 patients

	Bladder		Rectum		Uretha
	D2cc(%)	V75(cc)	D2cc(%)	V75(cc)	V125(cc)
I[a]	8.68 ± 1.06	0.48 ± 0.46	8.00 ± 1.01	0.19 ± 0.28	0.00 ± 0.01
II	8.67 ± 0.96	0.51 ± 0.34	8.24 ± 1.05	0.28 ± 0.34	0.03 ± 0.03
III	8.56 ± 0.97	0.46 ± 0.41	8.31 ± 1.09	0.31 ± 0.35	0.02 ± 0.02
P-values					
I *vs* II	0.758	0.796	0.039	0.168	0.001
I *vs* III	0.423	0.679	0.016	0.094	0.003
II *vs* III	0.756	0.421	0.918	0.998	0.856

[a]I, II and III are "Original", "Original Boost" and "Additional Boost" plans, respectively.

A similar study was previously implemented in the context of TRUS-based treatment planning to evaluate the feasibility of HDR focal boost.[23] Compared with the TRUS used in this previous study, CT images used in this study have superior image quality for contour delineation and image registration. Moreover, instead of rigid registration, a sophisticated deformable image registration is used in this study to address the anatomy difference between CT and MRI. In addition to dose comparison, the evaluation in this study takes further steps to the TCP and NTCP estimation to investigate the clinical impact of HDR boost plans.

The value of additional needles to achieve an optimal boost dose distribution was examined in this study. First, "Additional Boost" achieved higher TCP with less variation on DIL than "Original Boost" (Table 5), which implied better clinical performance with higher stability. Specifically, patients with EBRT obtained more benefit from "Additional Boost" than "Original Boost" (around 10%) compared to monotherapy patients (around 2%) (assuming α/β=3). Secondly, "Additional Boost" had less effect on original non-DIL prostate dose distribution than "Original Boost". In Table 3, compared with original plan, on average "Original Boost" showed 1% lower coverage and 1% higher hotspot on non-DIL prostate region with statistical significance, while "Additional Boost" showed no significant difference. It can be because that in order to escalate dose on DIL, several needles close to DIL would be re-optimized to be hotter to achieve the objective on DIL. It would increase optimization difficulty and inevitably sacrifice dose conformity in the remaining regions since parts of the prostate away from the DIL location needed to be cooled slightly to keep OAR constraints met, especially the urethra. This effect was decreased when an additional needle was added in or around the DIL which provided a more direct method of dose escalation and required much less dose contribution from the more distant original needles.

The additional time required for the whole procedure involving the additional boost needle is minimal. We estimated that the additional treatment time from the additional needle would be around 1–2 min, and the additional time in operation room (OR) would be 3 min in MR/TRUS guidance and 2 min in insertion of additional needles.

As discussed above, the TCP results demonstrated that patients treated by EBRT before HDR would obtain more benefit than monotherapy patients from focal DIL boost in HDR treatment. This is likely due to the fact that original monotherapy plans are able to achieve a higher total BED compared to EBRT combination plans and therefore achieve a greater TCP at baseline. Thus, it is further from the slope of the sigmoid curve about dose, and the same dose increment would lead to less improvement in TCP.

In the TCP modeling of this study, we chose the α/β ratio of prostate and DIL to be 1.5 Gy, 3 Gy and 10 Gy to evaluate the possibility of varying tumor radiation resistance. Although there is controversy regarding the α/β ratio for prostate cancer, most publications recommend α/β ratio between 1.5 and 3 Gy for prostate cancer,[44,45] and thus the TCP results of these corresponding α/β ratios are more clinically relevant.

The urethral dose constraints were met for all plans on this study despite boost dose escalation. In addition, the absolute values of urethra NTCP may be overestimated using the current parameters, given that they predict for higher rates of urethral stricture than what has been previously reported after brachytherapy or EBRT +brachytherapy (usually from 1.8 to 8.2%) in patient studies.[46–48] The potential reason can be that the parameters used in urethra NTCP LKB modeling, unlike those for bladder and rectum which are extensively studied and included in QUANTEC review,[49] lack enough support from solid clinical evidence. The parameters of urethra used in this study was extrapolated from Panettieri et al, where the source of these parameters is not provided.[43] Another publication also provides a set of NTCP LKB parameters of urethra without additional sources.[50] To the best of our knowledge, these are the only two publications presenting urethra NTCP LKB modeling parameters. Another important caveat is that given our assumption of urethral dose in the EBRT combination cohort, the reliability of the NTCP calculation may be affected and therefore should be viewed with caution.

CONCLUSIONS

In this study, we investigated the feasibility of mp-MRI-guided DIL boost in HDR prostate brachytherapy, and reported the clinical impact of this technique using TCP and NTCP estimation. Overall, with constraints maintained, boost plans with additional needles

Table 5. TCP and NTCP of different plans for patients with EBRT and without EBRT

		TCP, α/β=1.5 Gy		TCP, α/β=3 Gy		TCP, α/β=10 Gy	
		Prostate-DIL[a]	DIL	Prostate-DIL	DIL	Prostate-DIL	DIL
Patients with EBRT (8)	I[b]	89.3 ± 4.8	61.7 ± 28.5	85.2 ± 6.2	50.4 ± 33.2	63.3 ± 11.7	25.3 ± 33.0
	II	87.8 ± 4.9	83.6 ± 13.9	83.4 ± 6.1	75.9 ± 19.8	60.5 ± 11.5	45.8 ± 33.9
	III	87.4 ± 6.0	90.1 ± 7.5	83.1 ± 6.9	85.2 ± 11.3	60.7 ± 12.1	59.1 ± 27.1
	P-values						
	I *vs* II	0.250	0.008	0.195	0.016	0.250	0.008
	I *vs* III	0.469	0.016	0.469	0.016	0.297	0.016
	II *vs* III	0.297	0.031	0.219	0.031	0.219	0.031
Patients without EBRT (9)	I	94.8 ± 0.7	89.5 ± 16.9	91.1 ± 1.1	84.5 ± 21.0	70.8 ± 2.9	63.0 ± 25.3
	II	94.5 ± 1.1	96.1 ± 5.2	90.6 ± 1.6	93.5 ± 8.4	69.9 ± 4.1	80.3 ± 19.6
	III	94.3 ± 1.4	97.3 ± 3.0	90.3 ± 2.2	95.3 ± 5.2	69.0 ± 5.5	84.8 ± 14.9
	P-values						
	I *vs* II	0.258	0.004	0.250	0.004	0.426	0.004
	I *vs* III	0.219	0.004	0.301	0.004	0.359	0.004
	II *vs* III	0.805	0.008	0.734	0.008	0.652	0.008
		NTCP					
		Bladder		Rectum		Uretha	
Patients with EBRT (8)	I	10.5 ± 9.8		0		71.0 ± 2.1	
	II	11.1 ± 7.3		0		72.1 ± 1.8	
	III	8.5 ± 4.2		0		71.8 ± 1.8	
	P-values						
	I *vs* II	0.945		N/A		0.008	
	I *vs* III	0.938		N/A		0.016	
	II *vs* III	0.297		N/A		0.688	
Patients without EBRT (9)	I	0.1 ± 0.2		0		46.1 ± 5.9	
	II	0.5 ± 1.2		0		48.4 ± 6.3	
	III	0.2 ± 0.4		0		48.9 ± 6.9	
	P-values						
	I vs II	0.652		N/A		0.004	
	I vs III	0.570		N/A		0.008	
	II vs III	0.426		N/A		0.250	

[a]Prostate - DIL = Prostate with DIL cropped.
[b]I, II and III are "Original", "Original Boost" and "Additional Boost" plans, respectively.

around DILs were able to achieve V150 and V175 prescription coverage in 30% more DILs compared with boost plans using the original needle pattern. This was modeled to result in an increase in DIL TCP by 28% for patients with EBRT and by 8% for monotherapy patients compared with original plan. This retrospective study also suggested the use of mp-MRI-defined DIL to optimize needle placement may represent a strategy to personalize treatment delivery and improve tumor control.

ACKNOWLEDGMENTS

This research is supported in part by the National Cancer Institute of the National Institutes of Health under Award Number R01CA215718 (XY), the Department of Defense (DoD) Prostate Cancer Research Program (PCRP) Award W81XWH-13-1-0269 (XY), DoD W81XWH-17-1-0438 (TL) and W81XWH-17-1-0439 (AJ) and Dunwoody Golf Club Prostate Cancer Research Award, a philanthropic award provided by the Winship Cancer Institute of Emory University.

REFERENCES

1. Yoshioka Y. Current status and perspectives of brachytherapy for prostate cancer. *Int J Clin Oncol* 2009; **14**: 31–6. doi: https://doi.org/10.1007/s10147-008-0866-z
2. Peach MS, Trifiletti DM, Libby B. Systematic review of focal prostate brachytherapy and the future implementation of image-guided prostate HDR brachytherapy using MR-Ultrasound fusion. *Prostate Cancer* 2016; **2016**: 1–13. doi: https://doi.org/10.1155/2016/4754031
3. Scherr D, Swindle PW, Scardino PT. National comprehensive cancer network guidelines for the management of prostate cancer. *Urology* 2003; **61**(2 Suppl 1): 14–24. doi: https://doi.org/10.1016/S0090-4295(02)02395-6
4. Zaorsky NG, Doyle LA, Yamoah K, Andrel JA, Trabulsi EJ, Hurwitz MD, et al. High dose rate brachytherapy boost for prostate cancer: a systematic review. *Cancer Treat Rev* 2014; **40**: 414–25. doi: https://doi.org/10.1016/j.ctrv.2013.10.006
5. Yoshioka Y, Yoshida K, Yamazaki H, Nonomura N, Ogawa K. The emerging role of high-dose-rate (HDR) brachytherapy as monotherapy for prostate cancer. *J Radiat Res* 2013; **54**: 781–8. doi: https://doi.org/10.1093/jrr/rrt027
6. Chapman CH, Braunstein SE, Pouliot J, Noworolski SM, Weinberg V, Cunha A, et al. Phase I study of dose escalation to dominant intraprostatic lesions using high-dose-rate brachytherapy. *J Contemp Brachytherapy* 2018; **10**: 193–201. doi: https://doi.org/10.5114/jcb.2018.76881
7. Wise AM, Stamey TA, McNeal JE, Clayton JL. Morphologic and clinical significance of multifocal prostate cancers in radical prostatectomy specimens. *Urology* 2002; **60**: 264–9. doi: https://doi.org/10.1016/S0090-4295(02)01728-4
8. Arrayeh E, Westphalen AC, Kurhanewicz J, Roach M, Jung AJ, Carroll PR, et al. Does local recurrence of prostate cancer after radiation therapy occur at the site of primary tumor? Results of a longitudinal MRI and MRSI study. *Int J Radiat Oncol Biol Phys* 2012; **82**: e787–93. doi: https://doi.org/10.1016/j.ijrobp.2011.11.030
9. Dearnaley DP, Sydes MR, Graham JD, Aird EG, Bottomley D, Cowan RA, et al. Escalated-dose versus standard-dose conformal radiotherapy in prostate cancer: first results from the MRC RT01 randomised controlled trial. *Lancet Oncol* 2007; **8**: 475–87. doi: https://doi.org/10.1016/S1470-2045(07)70143-2
10. Gomez-Iturriaga A, Casquero F, Urresola A, Ezquerro A, Lopez JI, Espinosa JM, et al. Dose escalation to dominant intraprostatic lesions with MRI-transrectal ultrasound fusion High-Dose-Rate prostate brachytherapy. prospective phase II trial. *Radiother Oncol* 2016; **119**: 91–6. doi: https://doi.org/10.1016/j.radonc.2016.02.004
11. Rischke HC, Nestle U, Fechter T, Doll C, Volegova-Neher N, Henne K, et al. 3 tesla multiparametric MRI for GTV-definition of dominant Intraprostatic lesions in patients with prostate cancer – an interobserver variability study. *Radiat Oncol* 2013; **8**: 183–83. doi: https://doi.org/10.1186/1748-717X-8-183
12. Dickinson L, Ahmed HU, Allen C, Barentsz JO, Carey B, Futterer JJ, et al. Magnetic resonance imaging for the detection, localisation, and characterisation of prostate cancer: recommendations from a European consensus meeting. *European Urology* 2011; **59**: 477–94. doi: https://doi.org/10.1016/j.eururo.2010.12.009
13. Pinkawa M, Eble MJ, Mottaghy FM, . PET and PET/CT in radiation treatment planning for prostate cancer. *Expert Review of Anticancer Therapy* 2011; **11**: 1035–41. doi: https://doi.org/10.1586/era.11.51
14. Ling CC, Humm J, Larson S, Amols H, Fuks Z, Leibel S, et al. Towards multidimensional radiotherapy (MD-CRT): biological imaging and biological conformality. *Int J Radiat Oncol Biol Phys* 2000; **47**: 551–60. doi: https://doi.org/10.1016/S0360-3016(00)00467-3
15. Bauman G, Haider M, Van der Heide UA, Ménard C. Boosting imaging defined dominant prostatic tumors: a systematic review. *Radiother Oncol* 2013; **107**: 274–81. doi: https://doi.org/10.1016/j.radonc.2013.04.027
16. van Schie MA, Dinh CV, Houdt PJvan, Pos FJ, Heijmink SWTJP, Kerkmeijer LGW, et al. Contouring of prostate tumors on multiparametric MRI: evaluation of clinical delineations in a multicenter radiotherapy trial. *Radiother Oncol* 2018; **128**: 321–6. doi: https://doi.org/10.1016/j.radonc.2018.04.015
17. Monninkhof EM, van Loon JWL, van Vulpen M, Kerkmeijer LGW, Pos FJ, Haustermans K, et al. Standard whole prostate gland radiotherapy with and without lesion boost in prostate cancer: toxicity in the flame randomized controlled trial. *Radiother Oncol* 2018; **127**: 74–80. doi: https://doi.org/10.1016/j.radonc.2017.12.022
18. Zamboglou C, Thomann B, Koubar K, Bronsert P, Krauss T, Rischke HC, et al. Focal dose escalation for prostate cancer using ^{68}Ga-HBED-CC PSMA PET/CT and MRI: a planning study based on histology reference. *Radiat Oncol* 2018; **13**: 81. doi: https://doi.org/10.1186/s13014-018-1036-8
19. Brame RS, Zaider M, Zakian KL, Koutcher JA, Shukla-Dave A, Reuter VE, et al. Regarding the focal treatment of prostate cancer: inference of the Gleason grade from magnetic resonance spectroscopic imaging. *Int J Radiat Oncol Biol Phys* 2009; **74**: 110–4. doi: https://doi.org/10.1016/j.ijrobp.2008.07.055
20. Turkbey B, Albert PS, Kurdziel K, Choyke PL. Imaging localized prostate cancer: current approaches and new developments. *AJR Am J Roentgenol* 2009; **192**: 1471–80. doi: https://doi.org/10.2214/AJR.09.2527
21. Yang X, Rossi P, Mao H, Jani AB, Ogunleye T, Curran WJ, et al. A MR-TRUS registration method for ultrasound-guided prostate interventions. *SPIE Medical Imaging*. 2015: SPIE.
22. Yang X, Jani AB, Rossi PJ, Mao H, Curran WJ, Liu T. A MRI-CT prostate registration using sparse representation technique. *SPIE Medical Imaging*. 2016: SPIE.
23. Mason J, Al-Qaisieh B, Bownes P, Wilson D, Buckley DL, Thwaites D, et al. Multi-parametric MRI-guided focal tumor boost using HDR prostate brachytherapy: a feasibility study. *Brachytherapy* 2014; **13**: 137–45. doi: https://doi.org/10.1016/j.brachy.2013.10.011
24. Sun Y, Yuan J, Qiu W, Rajchl M, Romagnoli C, Fenster A. Three-dimensional nonrigid MR-TRUS registration using dual optimization. *IEEE Trans Med Imaging* 2015; **34**: 1085–95. doi: https://doi.org/10.1109/TMI.2014.2375207
25. Schmid M, Crook JM, Batchelar D, Araujo C, Petrik D, Kim D, et al. A phantom study to assess accuracy of needle identification in real-time planning of ultrasound-guided high-dose-rate prostate implants. *Brachytherapy* 2013; **12**: 56–64. doi: https://doi.org/10.1016/j.brachy.2012.03.002
26. Avants BB, Epstein CL, Grossman M, Gee JC. Symmetric diffeomorphic image registration with cross-correlation: evaluating automated labeling of elderly and neurodegenerative brain. *Med Image Anal* 2008; **12**: 26–41. doi: https://doi.org/10.1016/j.media.2007.06.004
27. Rueckert D, Sonoda LI, Hayes C, Hill DL, Leach MO, Hawkes DJ. Nonrigid registration using free-form deformations: application to breast MR images. *IEEE Trans Med Imaging* 1999; **18**: 712–21. doi: https://doi.org/10.1109/42.796284
28. Shen D, Davatzikos C. Hammer: Hierarchical attribute matching mechanism for elastic

registration. *IEEE Trans Med Imaging* 2002; **21**: 1421–39. doi: https://doi.org/10.1109/TMI.2002.803111
29. Vercauteren T, Pennec X, Perchant A, Ayache N. Diffeomorphic demons: efficient non-parametric image registration. *Neuroimage* 2009; **45**(1 Suppl): S61–S72. doi: https://doi.org/10.1016/j.neuroimage.2008.10.040
30. Yang X, Wu N, Cheng G, Zhou Z, Yu DS, Beitler JJ, et al. Automated segmentation of the parotid gland based on atlas registration and machine learning: a longitudinal MRI study in head-and-neck radiation therapy. *Int J Radiat Oncol Biol Phys* 2014; **90**: 1225–33. doi: https://doi.org/10.1016/j.ijrobp.2014.08.350
31. Yamada Y, Rogers L, Demanes DJ, Morton G, Prestidge BR, Pouliot J, et al. American brachytherapy Society consensus guidelines for high-dose-rate prostate brachytherapy. *Brachytherapy* 2012; **11**: 20–32. doi: https://doi.org/10.1016/j.brachy.2011.09.008
32. Fowler JF. Sensitivity analysis of parameters in linear-quadratic radiobiologic modeling. *Int J Radiat Oncol Biol Phys* 2009; **73**: 1532–7. doi: https://doi.org/10.1016/j.ijrobp.2008.11.039
33. Nag S, Gupta N. A simple method of obtaining equivalent doses for use in HDR brachytherapy. *Int J Radiat Oncol Biol Phys* 2000; **46**: 507–13. doi: https://doi.org/10.1016/S0360-3016(99)00330-2
34. Nahum A, Sanchez-NIeto B. Tumour control probability modelling: basic principles and applications in treatment planning. *Physica Medica* 2001; **17**(Suppl 2): 11.
35. Uzan J, Nahum AE. Radiobiologically guided optimisation of the prescription dose and fractionation scheme in radiotherapy using BioSuite. *Br J Radiol* 2012; **85**: 1279–86. doi: https://doi.org/10.1259/bjr/20476567
36. Murray LJ, Lilley J, Thompson CM, Cosgrove V, Mason J, Sykes J, et al. Prostate stereotactic ablative radiation therapy using volumetric modulated Arc therapy to dominant intraprostatic lesions. *Int J Radiat Oncol Biol Phys* 2014; **89**: 406–15. doi: https://doi.org/10.1016/j.ijrobp.2014.01.042
37. Nutting CM, Corbishley CM, Sanchez-Nieto B, Cosgrove VP, Webb S, Dearnaley DP. Potential improvements in the therapeutic ratio of prostate cancer irradiation: dose escalation of pathologically identified tumour nodules using intensity modulated radiotherapy. *Br J Radiol* 2002; **75**: 151–61. doi: https://doi.org/10.1259/bjr.75.890.750151
38. Kutcher GJ, Burman C. Calculation of complication probability factors for non-uniform normal tissue irradiation: the effective volume method. *Int J Radiat Oncol Biol Phys* 1989; **16**: 1623–30. doi: https://doi.org/10.1016/0360-3016(89)90972-3
39. Niemierko A. Reporting and analyzing dose distributions: a concept of equivalent uniform dose. *Med Phys* 1997; **24**: 103–10. doi: https://doi.org/10.1118/1.598063
40. Lyman JT. Complication probability as assessed from Dose-Volume histograms. *Radiation Research* 1985; **104**: S13–S19. doi: https://doi.org/10.2307/3576626
41. Burman C, Kutcher GJ, Emami B, Goitein M. Fitting of normal tissue tolerance data to an analytic function. *Int J Radiat Oncol Biol Phys* 1991; **21**: 123–35. doi: https://doi.org/10.1016/0360-3016(91)90172-Z
42. Michalski JM, Gay H, Jackson A, Tucker SL, Deasy JO. Radiation dose-volume effects in radiation-induced rectal injury. *Int J Radiat Oncol Biol Phys* 2010; **76**(3 Suppl): S123–S129. doi: https://doi.org/10.1016/j.ijrobp.2009.03.078
43. Panettieri V, Rancati T, Onjukka E, Smith RL, Ebert MA, Joseph DJ, et al. PV-0321: influence of urethra contouring on NTCP models predicting Urethral strictures in prostate HDRB. *Radiotherapy and Oncology* 2018; **127**: S170. doi: https://doi.org/10.1016/S0167-8140(18)30631-5
44. Kazi A, Godwin G, Simpson J, Sasso G. MRS-guided HDR brachytherapy boost to the dominant intraprostatic lesion in high risk localised prostate cancer. *BMC Cancer* 2010; **10**: 472. doi: https://doi.org/10.1186/1471-2407-10-472
45. Wang JZ, Guerrero M, Li XA, . How low is the alpha/beta ratio for prostate cancer? *Int J Radiat Oncol Biol Phys* 2003; **55**: 194–203. doi: https://doi.org/10.1016/S0360-3016(02)03828-2
46. Elliott SP, Meng MV, Elkin EP, McAninch JW, Duchane J, Carroll PR, et al. Incidence of urethral stricture after primary treatment for prostate cancer: data from CaPSURE. *J Urol* 2007; **178**: 529–34. doi: https://doi.org/10.1016/j.juro.2007.03.126
47. Díez P, Mullassery V, Dankulchai P, Ostler P, Hughes R, Alonzi R, et al. Dosimetric analysis of urethral strictures following HDR 192Ir brachytherapy as monotherapy for intermediate- and high-risk prostate cancer. *Radiother Oncol* 2014; **113**: 410–3. doi: https://doi.org/10.1016/j.radonc.2014.10.007
48. Hindson BR, Millar JL, Matheson B. Urethral strictures following high-dose-rate brachytherapy for prostate cancer: analysis of risk factors. *Brachytherapy* 2013; **12**: 50–5. doi: https://doi.org/10.1016/j.brachy.2012.03.004
49. Marks LB, Yorke ED, Jackson A, Ten Haken RK, Constine LS, Eisbruch A, et al. Use of normal tissue complication probability models in the clinic. *Int J Radiat Oncol Biol Phys* 2010; **76**(3 Suppl): S10–S19. doi: https://doi.org/10.1016/j.ijrobp.2009.07.1754
50. Gloi AM, Buchanan R. Dosimetric assessment of prostate cancer patients through principal component analysis (PCA). *J Appl Clin Med Phys* 2013; **14**: 40–9. doi: https://doi.org/10.1120/jacmp.v14i1.3882